Published in final edited form as:
BJU Int. 2012 October ; 110(7): 1062–1069. doi:10.1111/j.1464-410X.2012.10971.x.

Carbohydrate restriction and lactate transporter inhibition in a mouse xenograft model of human prostate cancer

Howard S. Kim[*,†], **Elizabeth M. Masko**[*], **Susan L. Poulton**[*], **Kelly M. Kennedy**[‡], **Salvatore V. Pizzo**[§], **Mark W. Dewhirst**[‡,§], and **Stephen J. Freedland**[*,†,§]

[*]Division of Urologic Surgery, Department of Surgery and the Duke Prostate Center, Duke University School of Medicine, Durham, NC, USA

[†]Urology Section, Veterans Affairs Medical Center, Durham, NC, USA

[‡]Department of Radiation Oncology and the Duke Comprehensive Cancer Center, Duke University School of Medicine, Durham, NC, USA

[§]Department of Pathology, Duke University School of Medicine, Durham, NC, USA

Abstract

- To determine if a no-carbohydrate ketogenic diet (NCKD) and lactate transporter inhibition can exert a synergistic effect on delaying prostate tumour growth in a xenograft mouse model of human prostate cancer.
- 120 nude athymic male mice (aged 6–8 weeks) were injected s.c. in the flank with 1.0 x 10^5 LAPC-4 prostate cancer cells.
- Mice were randomized to one of four treatment groups: Western diet (WD, 35% fat, 16% protein, 49% carbohydrate) and vehicle (Veh) treatment; WD and mono-carboxylate transporter-1 (MCT1) inhibition via α-cyano-4-hydroxycinnamate (CHC) delivered through a mini osmotic pump; NCKD (84% fat, 16% protein, 0% carbohydrate) plus Veh ; or NCKD and MCT1 inhibition.
- Mice were fed and weighed three times per week and feed was adjusted to maintain similar body weights.
- Tumour size was measured twice weekly and the combined effect of treatment was tested via Kruskal – Wallis analysis of all four groups. Independent effects of treatment (NCKD vs. WD and CHC vs. Veh) on tumour volume were tested using linear regression analysis.
- All mice were killed on Day 53 (conclusion of pump ejection), and serum and tumour sections were analysed for various markers. Again, combined and independent effects of treatment were tested using Kruskal – Wallis and linear regression analysis, respectively.
- There were no significant differences in tumour volumes among the four groups (P=0.09).
- When testing the independent effects of treatment, NCKD was significantly associated with lower tumour volumes at the end of the experiment (P=0.026), while CHC

Correspondence: Stephen Freedland, Division of Urology, Box 2626 DUMC, Duke University School of Medicine, Durham, NC 27710, USA. steve.freedland@duke.edu.

DISCLAIMER
Views and opinions of, and endorsements by the author(s) do not reflect those of the US Army or the Department of Defence.

administration was not (P=0.981). However, CHC was associated with increased necrotic fraction (P<0.001).

- Differences in tumour volumes were observed only in comparisons between mice fed a NCKD and mice fed a WD.
- MCT1 inhibition did not have a significant effect on tumour volume, although it was associated with increased necrotic fraction.

Keywords

prostate cancer; carbohydrate; ketogenic; lactate

INTRODUCTION

Prostate cancer is the most common non-cutaneous malignancy in men in the USA, with a lifetime incidence of one in six men. In 2010 alone, it is estimated that prostate cancer accounted for 28 percent of cancer incidences in men and 11 percent of cancer deaths [1]. To date, treatment has focused mainly on aggressive intervention, such as radical prostatectomy, brachytherapy, cryotherapy or hormonal therapy. Unfortunately, these interventions have significant side effects and are not always curative –especially for relapsed disease. Moreover, most men with prostate cancer ultimately succumb to other causes of mortality. There is therefore an increasing need to develop alternative, less toxic treatments for prostate cancer that not only slow tumour growth, but also improve overall health. As most prostate cancer deaths are attributable to castration-resistant prostate cancer (CRPC), we foresee three approaches to addressing this need: treat CRPC; prevent its development in the first place; or delay growth/progression of androgen-sensitive disease such that hormonal therapy is not needed or can be delayed, thus ultimately delaying the development of CRPC. In the present study we focus on delaying growth of androgen-sensitive disease, with the idea that this may ultimately have a great impact on prostate cancer morbidity and mortality without the need for hormonal therapy and all of its side effects. We do not envision that this approach will be curative, but hope that it can serve as a useful adjunct to standard treatments.

Freedland *et al.* [2] previously showed that a no-carbohydrate ketogenic diet (NCKD) delays prostate tumour growth and extends survival, relative to a traditional Western diet (WD) in a xenograft mouse model of human prostate cancer. These effects appear to be at least partly mediated by alterations in the IGF axis, as NCKD-fed mice present with lower serum insulin and IGF-1 levels than WD-fed mice. These findings support a growing body of literature arguing that insulin is a potent growth factor for prostate cancer cells *in vitro* [3], and that elevated serum insulin levels are directly associated with an increased epidemiological risk of prostate cancer [4].

Based on the results of this previous study, we hypothesized that decreased serum insulin may impair glucose delivery to tumour cells and place them in a *de facto* state of glucose deprivation. Given the metabolic demands of malignancy, impaired glucose uptake may thus represent a possible mechanism for the delay in prostate tumour growth observed in NCKD-fed mice. Indeed, previous work from Schroeder et al. [5] has shown that necrotic regions of tumour present with lower glucose concentration than surrounding tissue. However, direct glucose utilization is only one means by which tumour cells meet their metabolic needs. Recent work by Sonveaux et al. [6] has also demonstrated the existence of a unique symbiosis between hypoxic and aerobic cancer cells within a given tumour, with the aerobic cell type probably using lactate produced by the hypoxic cell type as a substrate for metabolism. The key regulatory agent in this symbiosis is mono-carboxylate transporter-1

(MCT1), a lactate influx transporter that is expressed in some aerobic cancer cell membranes and mitochondrial membranes. This suggests that inhibition of MCT1 may force aerobic cells to switch from lactate-fueled respiration to glycolysis, thereby depriving neighbouring hypoxic cells of adequate glucose and inducing cell death [7]. Given that prostate tumours have been shown to be significantly oxygen-deprived [8] and thus perhaps dependent on lactate uptake for energy, one would presume that prostate cancer cell lines would also demonstrate increased expression of MCT1.

The aforementioned studies extend a body of literature evidencing an O_2 and lactic acid gradient in tumours [9]. As distance from the nearest blood vessel increases, pO_2, pH and serum glucose decline in accordance with a cellular transition from aerobic respiration to anaerobic glycolysis. This metabolic reprogramming is orchestrated by hypoxia inducible factor-1 alpha (HIF-1α), a protein that, among other things, increases expression of the glucose influx transporter GLUT-1 in hypoxic cell membranes [10]. Prostate cancer cells, in particular, use HIF-1α as a key survival factor when subjected to serum deprivation [11].

In the present study, we investigated the combined anti-tumour efficacy of NCKD and MCT1 inhibition in a mouse xenograft model of human prostate cancer. We hypothesized that that these two mechanisms have the potential to work in concert to delay prostate tumour growth: a NCKD-induced decrease in serum insulin may impair glucose delivery to hypoxic cells, while MCT1 inhibition decreases lactate uptake in aerobic cells. Furthermore, lactate starvation in aerobic cells increases glucose consumption, thereby depriving hypoxic cells of metabolic substrate.

MATERIALS AND METHODS

In vitro studies

LAPC-4 human prostate cancer cells were obtained as a generous gift from William J. Aronson, UCLA School of Medicine, LA, USA. Cells were maintained in Iscove's Modified Medium with 10% fetal bovine serum and supplemented with 1nM androgen R1881. Cells were grown in 5% CO_2 at 37°C and harvested with HyQTase at 70–80% confluence in log-phase stage of growth.

Expression of MCT1 in four prostate cancer cell lines (CWR-22rv1, TRAMP-C1, LAPC-4, PC-3) and one immortalized non-neoplastic prostate cell line (RWPE) was determined by Western blot using rabbit anti-human primary antibody (AB3538P; Millipore, Billerica, MA, USA). Negative control was established before this study using identical reagents, using MDA-MB-231, a breast cancer cell line in which MCT1 is silenced via hypermethylation [6]. MCT1 expression was then confirmed by immunofluorescent staining, with rabbit anti-human MCT1 primary antibody (AB3538P; Millipore) and AlexaFluor 594 goat anti-rabbit secondary antibody (A21207; Invitrogen, Carlsbad, CA, USA), counterstained with DAPI nucleic acid stain. Image analysis was performed using a high-resolution solid-state camera mounted on a fluorescent microscope (Axioscop Zplus, Carl Zeiss, Inc.). Alexa594 fluorescence was detected using filter set at 555/568nm. DAPI was detected using a 4',6-diamindino-2-phenylindole filter.

Animal studies

We used a 2 x 2 factorial design with the following variables of interest: NCKD vs. WD, and MCT1 inhibition (via α-cyano-4-hydroxycinnamate [CHC]) vs. vehicle (Veh). The resulting treatment groups were: (1) NCKD/CHC; (2) WD/CHC; (3) NCKD/Veh; and (4) WD/Veh. The primary statistical outcome variable was tumour volume.

After obtaining approval from the Duke University Institutional Animal Care and Use Committee, 120 male nude athymic mice (Hsd: Athymic Nude-*Foxn1*^{Nu}, aged 6–8 weeks) were purchased from Harlan Laboratories (Indianapolis, IN, USA). Initially, a 30-day toxicity trial was conducted without tumour injection, comparing mouse response to three escalating concentrations of CHC (Sigma Life Sciences, St. Louis, MO, USA). All mice completed the trial without signs of morbidity. After a 7-day acclimation period, study mice were injected s.c. (Day 0) in the right flank with 1×10^5 LAPC-4 human prostate cancer cells suspended in 0.1mL Matrigel (Becton Dickinson, Franklin Lakes, NJ, USA).

On Day 11, mice were randomized to receive either 9.5uM/day CHC or Veh (50/50 DMSO/PEG), delivered via mini-osmotic pump (Alzet Corporation, Cupertino, CA, USA). Using sterile technique and isofluorane anaesthetic, a small incision was made over the left flank to insert the pump, and the wound was closed with 9mm clips and treated with triple antibiotic ointment. On Day 13, mice were again randomized to either a NCKD (kcal 84% fat, 16% protein, 0% carbohydrate) or WD (kcal 35% fat, 16% protein, 49% carbohydrate) prepared by TestDiet (Indianapolis, IN, USA) as previously described [2].

Based on observations from the toxicity trial, mice receiving NCKD were fed *ad libitum* while mice receiving WD were feed-restricted to maintain equivalent weights amongst all four groups. All mice were fed and weighed thrice weekly. When tumours became palpable, a single operator (H.S.K.) measured dimensions using digital calipers for the duration of the study. Tumour volume was determined using the following formula: width x height x length x 0.5235 [12].

All mice were killed after completion of pump ejection (Day 53). The mice were anaesthetized with sodium pentobarbital (85mg/kg), and tumours were excised, snap-frozen in liquid nitrogen, and stored at -80°C. Histological and immunofluorescent analyses were performed on the median 9–10 tumours per group. At the time of death, mice underwent thoracotomy and were exsanguinated via cardiac puncture, after which sera were isolated and stored at −20°C for further analyses.

Immunofluorescent staining

Tumours were sliced into 10-μm sections using a LEICA CM 1850 cryotome (Meyer Instruments Inc., Houston, TX, USA) maintained at -24°C to −28°C. Vasculature was identified with CD-31 staining using rat anti-mouse primary antibody (553708; Becton Dickinson Biosciences) and goat anti-rat AlexaFluor 488 secondary antibody (A11006; Invitrogen). In brief, sections were thawed at room temperature and fixed in cold methanol (−20° C) for 30 min, followed by blocking for 30 min at room temperature with 5% donkey serum in primary antibody dilution buffer (PADB; Biomeda, Foster City, CA, USA). Sections were stained with primary antibody (1:100 in PADB) for 1 h and secondary antibody (1:1,000 in PADB) for 1 h, then briefly counterstained with Hoescht working solution (0.1g/5mL 0.9% saline) for 5 min. Between each of the aforementioned steps, all sections were washed in triplicate with 1x PBS. Specimens were stored in 4% formalin and immediately imaged using a filter set at 494/518nm. Images were saved and vessels per unit area of 1.5857 mm^2 were counted using Adobe Photoshop (San Jose, CA, USA).

Tumour necrosis score

Tumours were sliced into 20-μm sections, as described previously. Sections were stained with haematoxlyin and eosin to identify tissue architecture, then scored by a board-certified pathologist (S.V.P.) blinded to treatment group for percent necrosis, as a function of total tumour area.

Tumour lysate

Tumour tissue was sliced into 10-μm sections and homogenized via Qproteome Mammalian Protein Prep Kit (Qiagen, Germantown, MD, USA). Total protein concentration was determined and standardized using a BCA assay (Thermo Scientific, Rockford, IL, USA). Tumour lysates were measured for HIF-1α concentration via ELISA (R&D Systems, Minneapolis, MN).

Serum analysis

Sera from the median 9–10 mice per group were assayed for insulin (Millipore), IGF-I, and IGFBP-3 (R&D Systems) using mouse-specific ELISAs. Serum measurements for lactate (Beckman, Fullerton, CA, USA), total ketones, and 3-hydroxybutyrate (Wako USA, Richmond, VA, USA) were performed using a Beckman DxC600 auto-analyzer. Blood glucose was measured after the mice were killed, using a hand-held Ascensia Contour glucometer (Bayer Healthcare, Tarrytown, NY, USA).

Statistical analysis

The StataR11 software package (StataCorp; College Station, TX) was used for all statistical analysis. Overall trends in tumour volume, body weight, calorific intake, percent tumour necrosis, serum lactate, glucose, ketones and insulin were analysed using a Kruskal–Wallis test. The primary outcome of tumour volume was further evaluated among pairs using rank-sum analysis. As this was a cross-sectional study with all mice killed at the same time, we also wanted to evaluate differences in earlier tumour growth among arms. To accomplish this we used Kaplan –Meier analysis, with survival being defined as time from tumour injection until the tumour volume reached $100mm^3$.

To analyse the independent effect of either treatment, we re-distributed mice into two groups – one to indicate assignment to either a NCKD or WD, and another to indicate assignment to either CHC or Veh – and performed linear regression analysis with tumour volume as the outcome variable. All *P* values were two-sided and a *P* value of <0.05 was considered to indicate statistical significance.

RESULTS

Confirmation of MCT1 expression

All five cell lines expressed MCT1, as shown by Western blot analysis (Fig. 1). MCT1 expression was confirmed and found to be heavily expressed in the cell periphery via immunofluorescent microscopy (Fig. 2).

Body weight and calorific intake

Median body weights did not significantly differ among the groups over the course of the study (Fig. 3A, all $P>0.21$). Median body weight for all groups was 30.9g at randomization (Day 11) and 33.0g at the conclusion of the study (Day 53). As described previously, mice receiving WD were feed-restricted to maintain similar body weights to mice receiving NCKD, who were fed *ad libitum*. As a result, there was significant variation in calorific intake among the groups, with mice receiving WD consuming 20--50% fewer calories daily than mice receiving NCKD over the course of the study (Fig. 3B).

Tumour growth

Tumour growth curves are shown in Fig. 4A. The initial day of tumour palpability was earliest in the double control group (WD/Veh, Day 25) and latest in the double treatment group (NCKD/CHC, Day 32). At the end of the study on Day 53, overall comparison of

tumour volumes between the groups had trended towards, but did not reach, statistical significance (Kruskal – Wallis, P=0.09). Tumour volume distribution, by group, at the end of the study is shown in Fig. 4B. Mice from the double control group (WD/Veh) had the largest median tumour volume (190.9mm^3), while mice from the double treatment group (NCKD/CHC) had the smallest median tumour volume (82.6mm^3). Median tumour volumes for the single treatment groups, WD/CHC and NCKD/Veh, were 175.5mm^3 and 144.8mm^3, respectively.

Kaplan – Meier survival analysis is shown in Fig. 5. Notably, the NCKD groups (with or without CHC) clustered together and have been separated from the WD groups (with or without CHC) for ease of observation.

After redistributing mice into variables defined by either NCKD vs. WD or CHC vs. Veh, linear regression analysis showed that NCKD was significantly associated with lower tumour volumes when the mice were killed (P=0.026), while CHC administration was not (P=0.981). Only one pairwise comparison, NCKD/CHC vs. WD/CHC, was significant (P=0.05). Although no other pairwise comparisons were significant, all permutations pairing NCKD vs. WD approached significance (P=0.09, P=0.14, P=0.23).

Tumour necrosis

Percent necrosis differed significantly among the groups (Fig. 6; Kruskal – Wallis, P<0.001). In linear regression analysis, CHC administration was independently associated with increased necrosis (P<0.001), while NCKD treatment was not (P=0.58). However, this observation was driven by very little necrosis in the NCKD/Veh arm. Indeed, the NCKD/Veh arm had lower necrosis than all three other groups (all P 0.001), whereas the other three groups did not differ (all P>0.30).

Tumour CD31 and HIF-1α

Microvessel density, as measured by CD31 staining (Fig. 7), differed significantly among the groups (Fig. 7; Kruskal – Wallis, P<0.001). This trend was driven by the high microvessel density of the WD/Veh group, for which all pairwise comparisons were significant (all P<0.05). Tumour HIF-1α content also differed significantly among the groups (Fig. 8; Kruskal–Wallis, P=0.02), although this trend was driven by the relatively low value of the WD/Veh group. On linear regression, neither CHC nor NCKD was found to be predictive of vasculature score or HIF-1α content.

Serum analyses

Serum lactate levels at the end of the study differed significantly among treatment groups (Fig. 9A; Kruskal–Wallis, P=0.006), as did serum ketones levels (Fig. 9B; P=0.02). However, neither independent treatment was found to be associated with serum lactate (both P>0.13) or ketones (both P>0.10).

Serum glucose did not differ significantly among treatment groups (Fig. 9C; P=0.27), nor did serum insulin (Fig. 9D; P=0.06), IGF-1 (Fig. 9E; P=0.72), or IGFBP-3 (Fig. 9F; P=0.82). Subsequent linear regression analyses did not show any independent effects of treatment on serum glucose, insulin, IGF-1 or IGFBP-3 (all P>0.2).

DISCUSSION

The MCT1 lactate transporter is well characterized in the tumour physiology of several malignancies, including breast, ovarian, colorectal and lung carcinoma [6, 13, 14]. In the present study, we confirmed the expression of MCT1 in four prostate cancer cell lines and

one immortalized non-neoplastic prostate cell line (Figs 1 and 2). Previous studies have shown expression of MCT1 in the PC-3 cell line [6, 15]; however, we showed that MCT1 is expressed in four other commonly investigated prostate cell lines: RWPE, CWR-22rv1, TRAMP-C, and LAPC-4.

Based on previous studies, we aimed to investigate the combined anti-tumour efficacy of a NCKD and MCT1 inhibition (CHC) in a mouse xenograft model of human prostate cancer. We hypothesized that a NCKD and lactate transporter inhibition would demonstrate a synergistic anti-tumour effect, with combined therapy delaying tumour growth more substantially than either therapy alone.

On gross examination of our results, we found this hypothesis to be accurate, with tumours from the double treatment group (NCKD/CHC) exhibiting the smallest median tumour volumes, compared with both single treatment groups (NCKD/Veh and WD/CHC) and the double control group (WD/Veh). However, comparison of all four groups did not reach statistical significance (Fig. 4A; P=0.09). Kaplan–Meier survival analysis, with an endpoint defined as a tumour volume of 100mm^3, did not reach statistical significance either (Fig. 5; P=0.16), but the survival curve does show the emergence of two different survival trajectories, with the two groups containing the ketogenic diet (NCKD/CHC and NCKD/Veh) expressing a similar rate of ‘survival’, which was prolonged compared with the two groups receiving WD (WD/CHC and WD/Veh); these also had similar ‘survival’ regardless of CHC or Veh. These results point to an independent effect of dietary restriction on tumour growth, but not CHC.

As a result, we tested the independent effect of each treatment (NCKD vs. WD and CHC vs. Veh) on tumour volume using linear regression analysis. We found that only a NCKD (vs. WD) was significantly associated with lower tumour volumes (P=0.026), while CHC administration (vs. Veh) had no effect on tumour volume (P=0.98).

This result confirms the findings of a previous study by Freedland *et al.* [2], which found that a NCKD delayed prostate tumour growth relative to a WD. There are, however, several important differences between that study and the present study. Most notably, the present study added a second treatment variable of CHC, which we found to have no significant effect on tumour growth. Additionally, the previous study randomized mice to dietary treatment groups 24 days *before* tumour inoculation, while the present study randomized mice to treatment groups 11 days *after* tumour inoculation. Thus, the earlier study addressed a question of prevention while the present study addressed a question of treatment after tumour initiation [16], so it is difficult to compare across studies, and it would require a separate study to test whether treatment before or after tumour inoculation influences the efficacy of MCT1 inhibition.

The present findings regarding MCT1 inhibition alone fail to confirm those presented by Sonveaux et al. [6], which found a significant association between MCT1 inhibition and delayed tumour growth *in vivo*, as well as a compelling explanation for the efficacy of MCT inhibition based on *in vitro* data. Our limited application of their *in vivo* findings did not reproduce a similar result of tumour growth restriction, although the possible explanations for this discrepancy are many. To begin with, the present study administered CHC at a continuous rate through pump infusion, while previous investigations administered daily CHC boluses through i.p. injections. Additionally, it is possible that a study with a longer duration would have produced a significant effect on tumour volume, as the data were trending in that direction. Unfortunately, the study was pre-determined to conclude on Day 53 owing to the conclusion of pump ejection. Finally, we did find that CHC was independently associated with increased tumour necrotic fraction and dramatically increased

necrosis when combined with the NCKD compared to the NCKD/Veh arm. Thus, while CHC did not exert a significant effect on our primary outcome of tumour volume, this does not rule out the possibility of MCT1 inhibition as a useful adjunct in the treatment of prostate cancer.

Given the significant independent effect of NCKD on tumour volume, we examined several serum markers of the insulin growth factor axis in an effort to explain our findings. In our previous study, we observed that mice fed a WD had significantly higher levels of serum insulin than mice fed a NCKD [2], supporting the well-established theory that insulin may serve as a mitogen for prostate cancer. In the present study, however, we did not find any significant differences in serum insulin, IGF-1, IGFBP-3, or glucose. This suggests that there may be pathways beyond the IGF axis that may mediate the anti-growth properties of a NCKD in established tumours.

We also examined serum levels of ketones and lactate amongst the groups, finding both of these to be significantly different among groups. Mice receiving CHC treatment (NCKD/CHC and WD/CHC) had lower serum ketone levels than mice receiving Veh (NCKD/Veh and WD/Veh, Fig. 9B). This is probably attributable to the fact that CHC also inhibits pyruvate influx across the mitochondrial membrane [17], thereby preventing pyruvate conversion to acetyl-coA, a vital component of ketone body synthesis.

Compared with the double control group (WD/Veh), all other groups had elevated serum lactate levels. Although this was expected in mice receiving CHC, as CHC inhibits lactate influx and utilization, it is unclear why mice in the NCKD/Veh group also had elevated serum levels of lactate. One explanation may be found in the decreased microvessel density of the NCKD/Veh group (Fig. 7), consistent with previous findings in energy-restricted mice burdened with xenograft prostate tumours [18]. As tumour angiogenesis directly correlates with tissue oxygenation, it is plausible that these tumours were relatively hypoxic and therefore favoured lactate production via glycolysis. Ultimately, the exact reason for this observation is unclear and requires further study.

On histological examination of tumour sections, there was a significant difference in the extent of necrosis between the treatment groups (Fig. 6; $P<0.001$). Based on previous work with MCT1 inhibition [6], we hypothesized that necrosis scores in mice receiving CHC would be increased relative to mice receiving vehicle owing to the limitation of lactate as a metabolic substrate. Indeed, both treatment groups receiving CHC demonstrated high degrees of necrosis (Fig. 6), and we observed a significant independent effect of CHC on necrosis ($P<0.001$). This effect was particularly pronounced in comparison with the NCKD/Veh group, which exhibited a significantly lower degree of necrosis – consistent with a slow-growing, well-vascularized tumour (Fig. 7). However, we also observed an unexpectedly high degree of necrosis in the WD/Veh group. This observation may be explained by the relatively faster rate of tumour growth of the WD/Veh group (Fig. 4), as these tumours tended to be poorly vascularized (Fig. 7).

We also examined tumour homogenate for expression of HIF-1α. Compared with the WD/Veh group, tumours from mice in all other groups expressed higher levels of HIF-1α. The trend in these data closely mirrors that of serum lactate levels among the groups, which is not surprising given that lactate reflects a preference for anaerobic glycolysis over aerobic oxidative phosphorylation. Additionally, previous research has shown that lactate may actually stabilize HIF-1α and prevent its degradation [19].

It should be noted that the present study did not address a castrate-resistant model of prostate cancer – the pivotal menace of prostate disease. We chose a non-castrate model because of the many side effects associated with castration in an animal model. Thus, the goal of the

present study was to assess whether diet and lactate inhibition, as adjuvant therapy, could slow growth sufficiently to delay the need for androgen deprivation in the first place. However, we do acknowledge that castration resistance is an important area for future research.

In summary, the primary goal of the study was to determine whether the addition of MCT1 inhibition to carbohydrate restriction delayed tumour growth relative to either therapy alone. Given the negative finding of synergy, additional mechanistic studies were not performed. Our results do confirm the finding that a NCKD delays prostate tumour growth in a xenograft mouse model of human prostate cancer. However, dietary intervention should be regarded as an adjuvant and not the main therapeutic measure against prostate cancer. Unfortunately, we did not find an association between MCT1 inhibition and tumour growth restriction or any evidence of synergistic effect between diet and MCT1 inhibition.

Acknowledgments

Supported by the Department of Veterans Affairs, the American Urological Association Foundation/Astellas Rising Star in Urology Award, NIH 5R01-CA131235-02 (SJF), and the Howard Hughes Medical Institute (HSK).

Abbreviations

NCKD	no-carbohydrate ketogenic diet
WD	Western diet
Veh	vehicle
CHC	α-cyano-4-hydroxycinnamate
CRPC	castration-resistant prostate cancer
MCT1	mono-carboxylate transporter-1
HIF-1α	hypoxia inducible factor-1-α
PADB	primary antibody dilution buffer

References

1. Jemal A, Siegel R, Xu J, Ward E. Cancer statistics, 2010. CA: a cancer journal for clinicians. 2010 Sep-Oct;60:277–300. [PubMed: 20610543]
2. Freedland SJ, Mavropoulos J, Wang A, et al. Carbohydrate restriction, prostate cancer growth, and the insulin-like growth factor axis. Prostate. 2008 Jan 1.68:11–9. [PubMed: 17999389]
3. Tymchuk CN, Barnard RJ, Ngo TH, Aronson WJ. Role of testosterone, estradiol, and insulin in diet- and exercise-induced reductions in serum-stimulated prostate cancer cell growth in vitro. Nutr Cancer. 2002; 42:112–6. [PubMed: 12235642]
4. Roddam AW, Allen NE, Appleby P, et al. Insulin-like growth factors, their binding proteins, and prostate cancer risk: analysis of individual patient data from 12 prospective studies. Ann Intern Med. 2008 Oct 7.149:461–71. W83–8. [PubMed: 18838726]
5. Schroeder T, Yuan H, Viglianti BL, et al. Spatial heterogeneity and oxygen dependence of glucose consumption in R3230Ac and fibrosarcomas of the Fischer 344 rat. Cancer Res. 2005 Jun 15.65:5163–71. [PubMed: 15958560]
6. Sonveaux P, Vegran F, Schroeder T, et al. Targeting lactate-fueled respiration selectively kills hypoxic tumor cells in mice. J Clin Invest. 2008 Dec.118:3930–42. [PubMed: 19033663]
7. Moeller BJ, Dreher MR, Rabbani ZN, et al. Pleiotropic effects of HIF-1 blockade on tumor radiosensitivity. Cancer Cell. 2005 Aug.8:99–110. [PubMed: 16098463]
8. Movsas B, Chapman JD, Horwitz EM, et al. Hypoxic regions exist in human prostate carcinoma. Urology. 1999 Jan.53:11–8. [PubMed: 9886581]

9. Helmlinger G, Yuan F, Dellian M, Jain RK. Interstitial pH and pO2 gradients in solid tumors in vivo: high-resolution measurements reveal a lack of correlation. Nat Med. 1997 Feb.3:177–82. [PubMed: 9018236]
10. Ebert BL, Firth JD, Ratcliffe PJ. Hypoxia and mitochondrial inhibitors regulate expression of glucose transporter-1 via distinct Cis-acting sequences. J Biol Chem. 1995 Dec 8.270:29083–9. [PubMed: 7493931]
11. Thomas R, Kim MH. HIF-1 alpha: a key survival factor for serum-deprived prostate cancer cells. Prostate. 2008 Sep 15.68:1405–15. [PubMed: 18563715]
12. Thomas JA 2nd, Antonelli JA, Lloyd JC, et al. Effect of intermittent fasting on prostate cancer tumor growth in a mouse model. Prostate cancer and prostatic diseases. 2010 Dec.13:350–5. [PubMed: 20733612]
13. Pinheiro C, Reis RM, Ricardo S, Longatto-Filho A, Schmitt F, Baltazar F. Expression of monocarboxylate transporters 1, 2, and 4 in human tumours and their association with CD147 and CD44. J Biomed Biotechnol. 2010; 2010:427694. [PubMed: 20454640]
14. Pinheiro C, Albergaria A, Paredes J, et al. Monocarboxylate transporter 1 is up-regulated in basal-like breast carcinoma. Histopathology. 2010 Jun.56:860–7. [PubMed: 20636790]
15. Hao J, Chen H, Madigan MC, et al. Co-expression of CD147 (EMMPRIN), CD44v3-10, MDR1 and monocarboxylate transporters is associated with prostate cancer drug resistance and progression. Br J Cancer. 2010 Aug 24.
16. Mavropoulos JC, Isaacs WB, Pizzo SV, Freedland SJ. Is there a role for a low-carbohydrate ketogenic diet in the management of prostate cancer? Urology. 2006 Jul.68 :15–8. [PubMed: 16844447]
17. Halestrap AP. The mitochondrial pyruvate carrier. Kinetics and specificity for substrates and inhibitors. Biochem J. 1975 Apr.148:85–96. [PubMed: 1156402]
18. Mukherjee P, Sotnikov AV, Mangian HJ, Zhou JR, Visek WJ, Clinton SK. Energy intake and prostate tumor growth, angiogenesis, and vascular endothelial growth factor expression. J Natl Cancer Inst. 1999 Mar 17.91:512–23. [PubMed: 10088621]
19. Lu H, Dalgard CL, Mohyeldin A, McFate T, Tait AS, Verma A. Reversible inactivation of HIF-1 prolyl hydroxylases allows cell metabolism to control basal HIF-1. J Biol Chem. 2005 Dec 23.280:41928–39. [PubMed: 16223732]

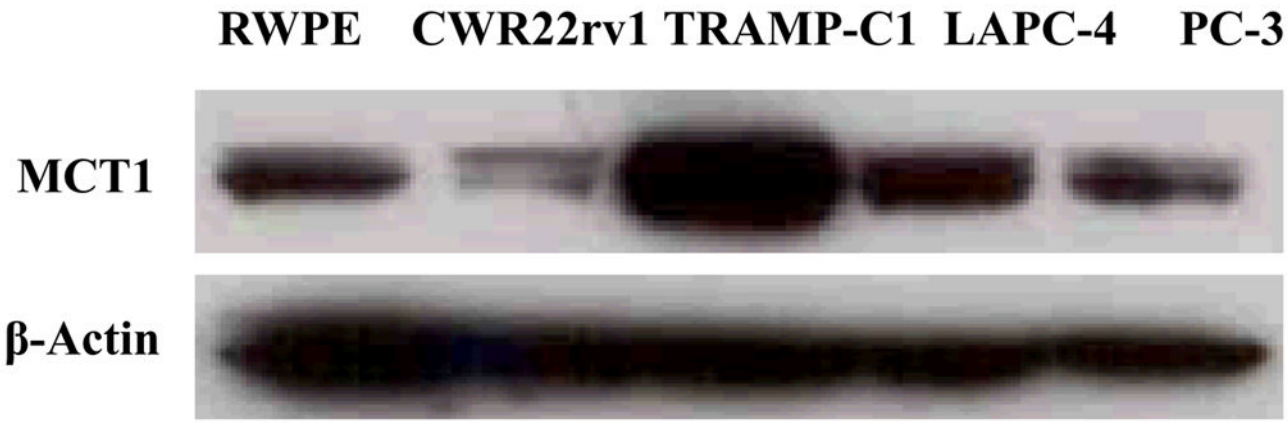

Fig 1.

Western blot analysis shows the presence of MCT1 (~45 kDa) in all five prostate cell lines of interest. Positive control is β-Actin. Negative control was established in a previous study, using the MDA-MB-231 breast cancer cell line [6].

CWR22rv1

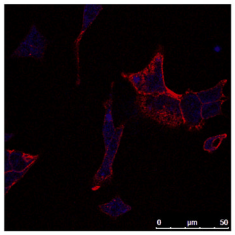

LAPC4

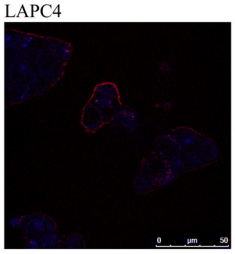

PC3

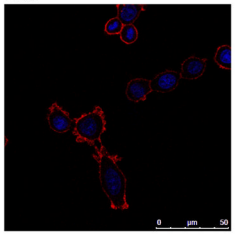

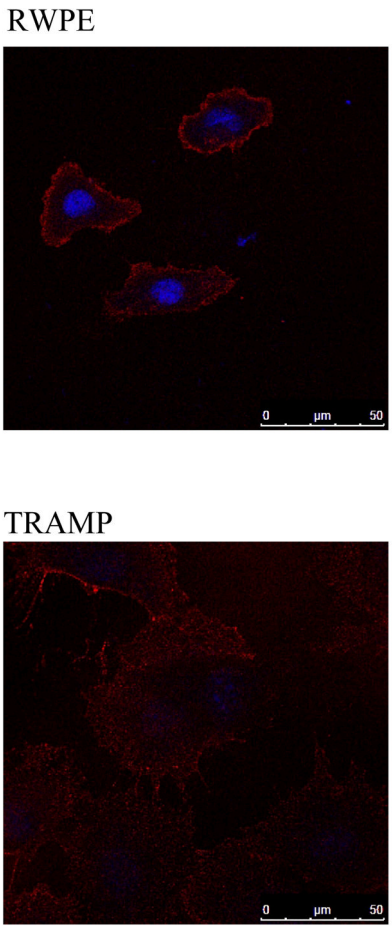

Fig. 2.
Immunofluorescent microscopy confirms the presence of MCT1 (red) in all five prostate cell lines of interest, localized primarily to the cell periphery. DAPI nucleic acid counterstain is shown in blue.

A

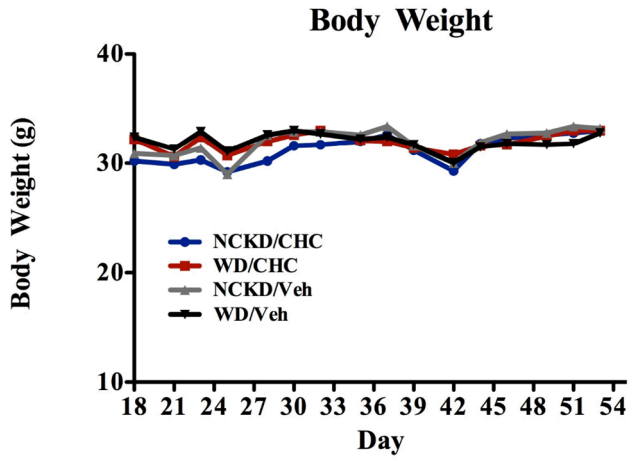

B

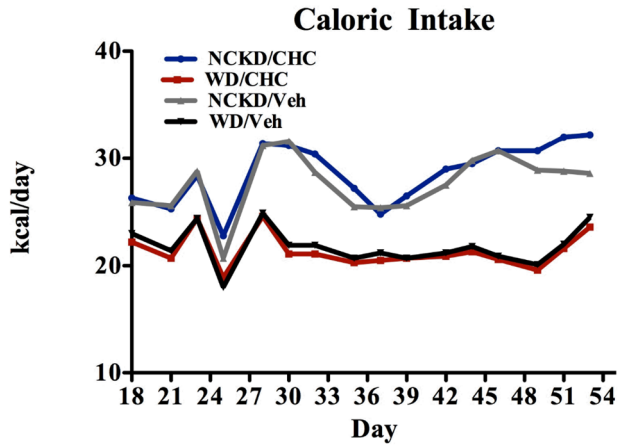

Fig. 3.

A, Body weight vs. study day by group. **B**, Calorific intake vs. study day by group.

A

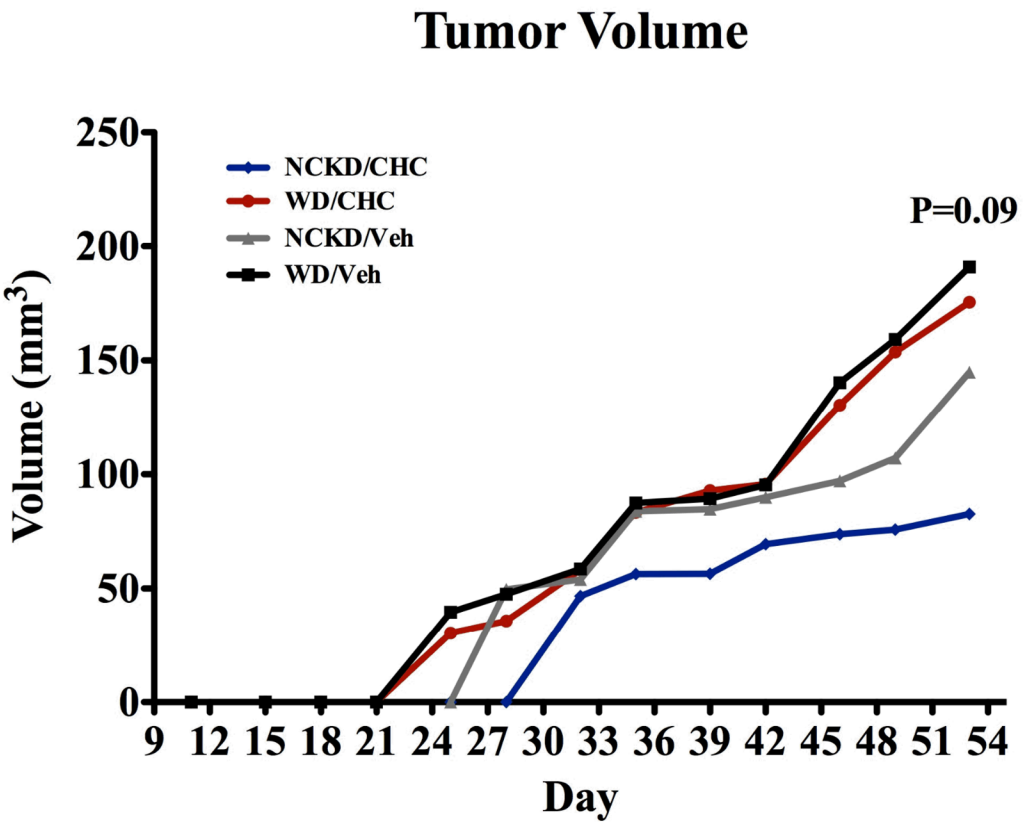

B

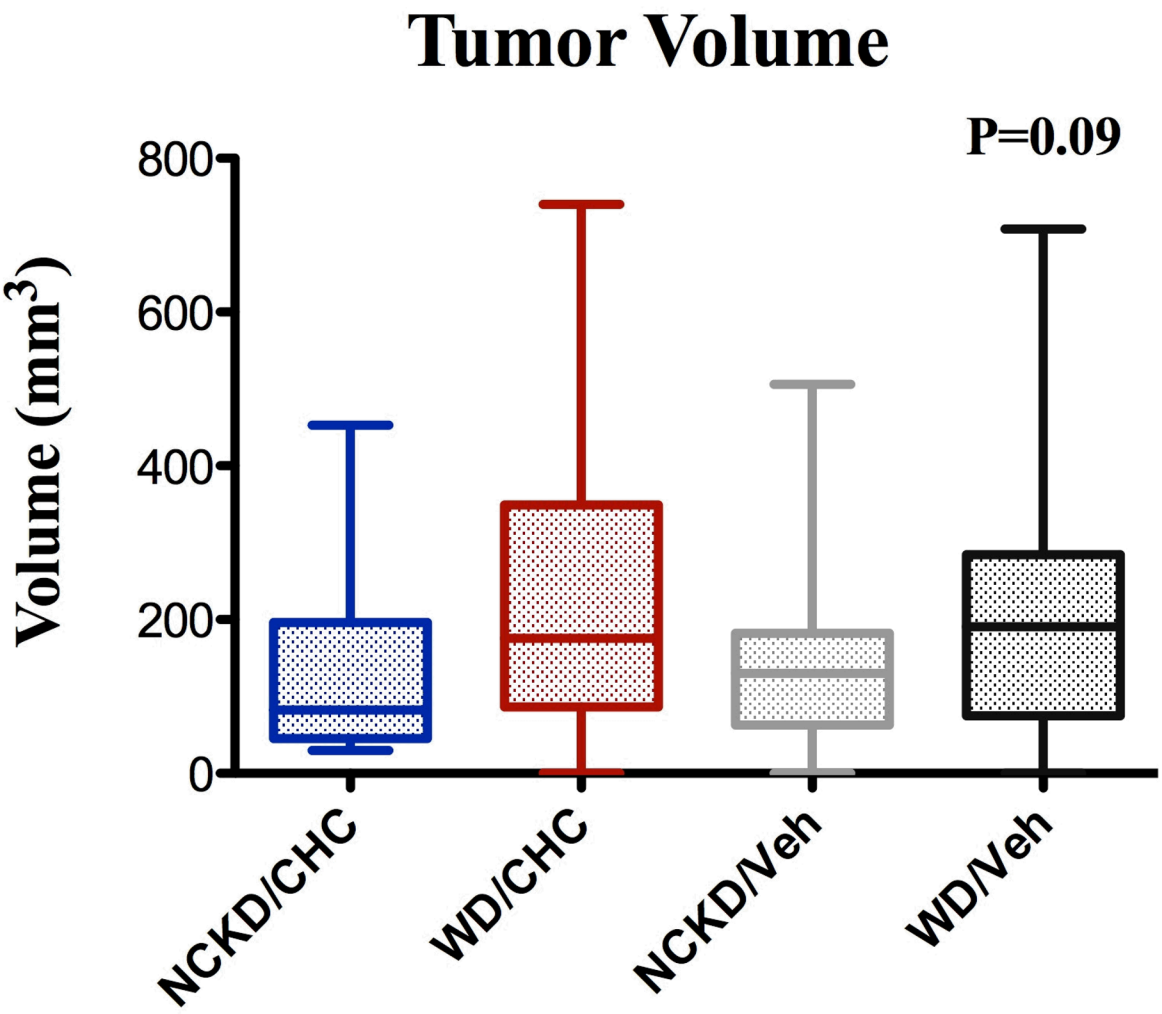

Fig. 4.

LAPC-4 xenograft tumour growth in nude, athymic mice. **A**, Tumour volumes by group. **B**, Tumour volumes when the mice were killed (Day 53). Box represents 25th, 50th, and 75th percentile. Whisker represents 5th and 95th percentile.

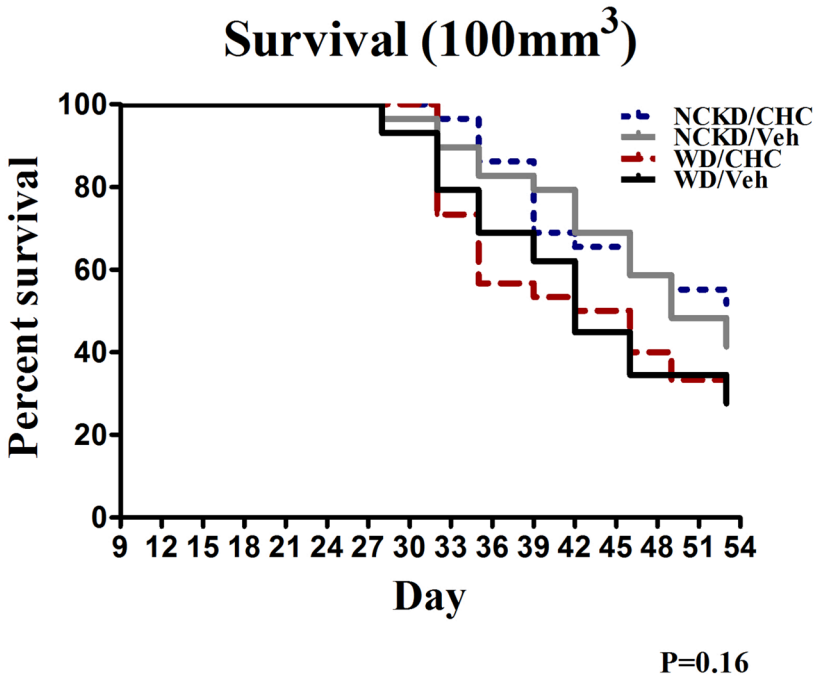

Fig. 5.
Kaplan – Meier survival analysis, defined as number of days until tumour volume reached 100mm^3.

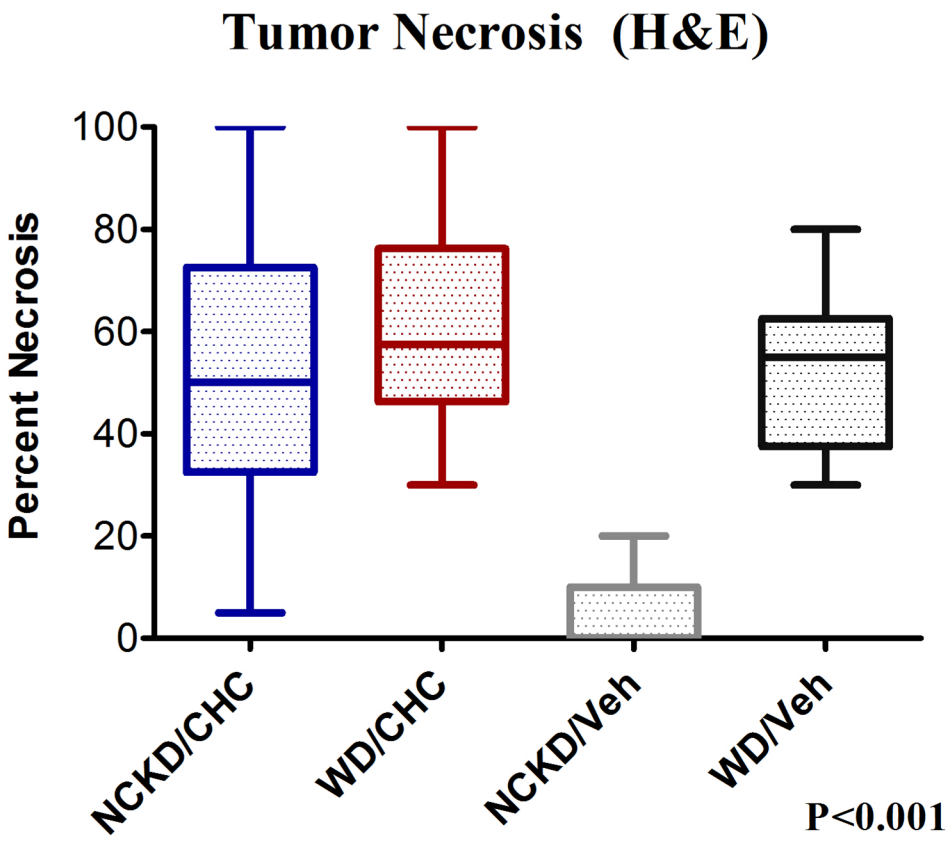

Fig. 6.

Percent necrosis when the mice were killed (Day 53), determined by analysis of haematoxylin and eosin stained slides by a board-certified pathologist. Box represents 25th, 50th, and 75th percentile. Whisker represents 5th and 95th percentile.

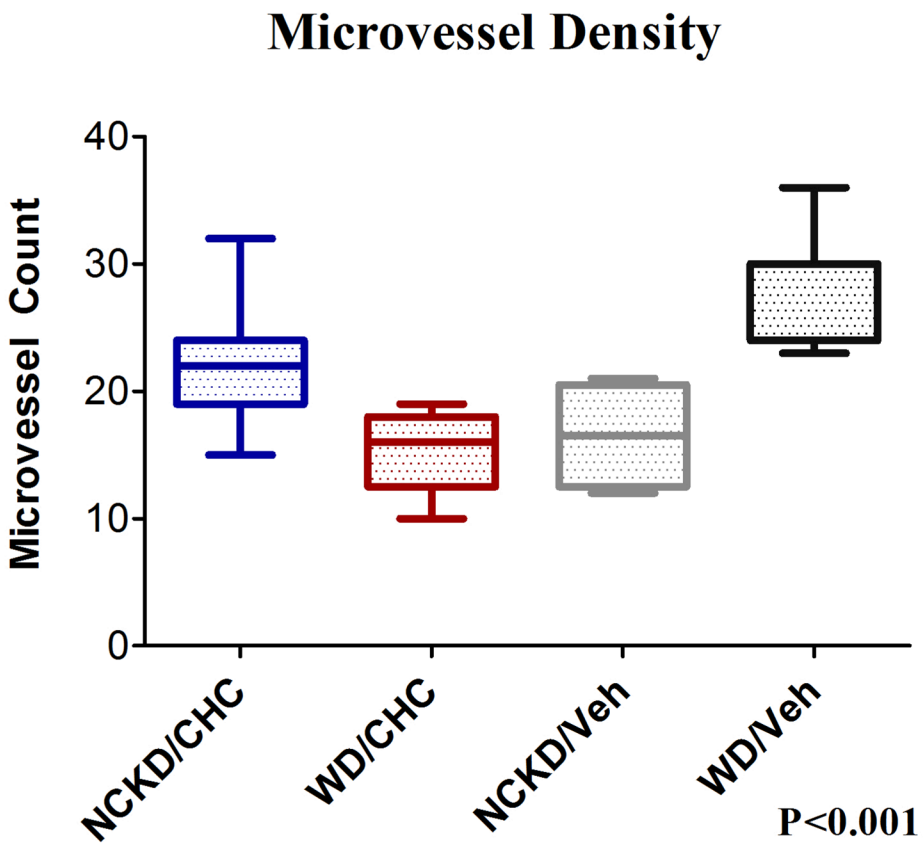

Fig. 7.
Microvessel density when the mice were killed (Day 53), determined by CD31 immunofluroescence staining. The number of vessels per 1.5857 mm^2 were manually counted.

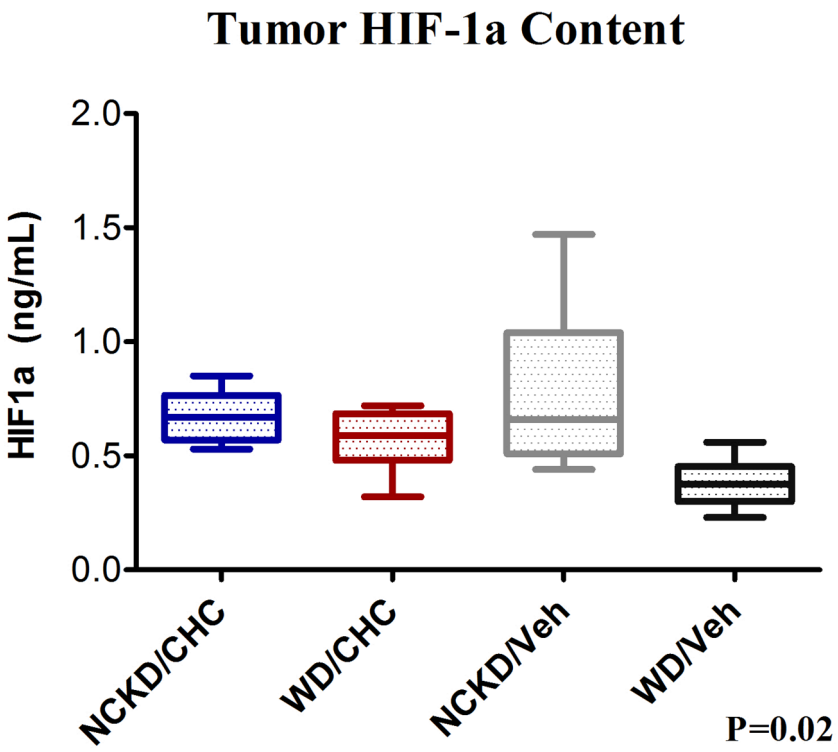

Fig. 8.
Tumour HIF-1a content when the mice were killed (Day 53), determined by ELISA of tumour homogenate.

A

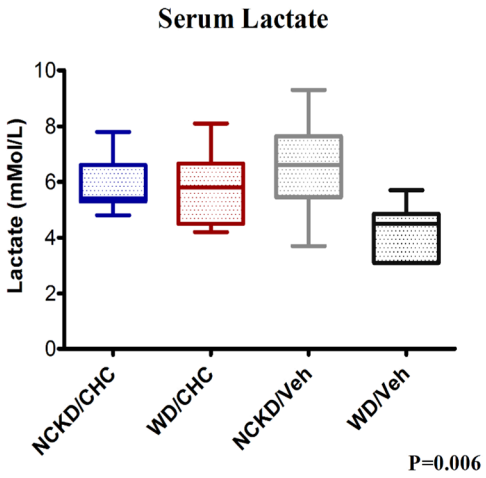

B

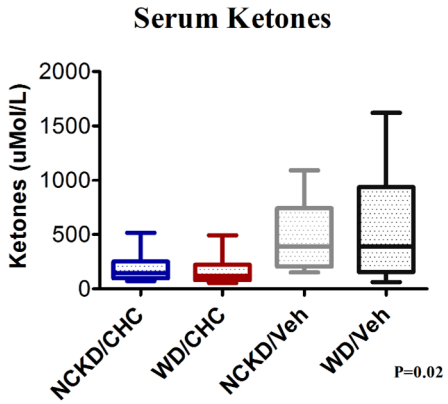

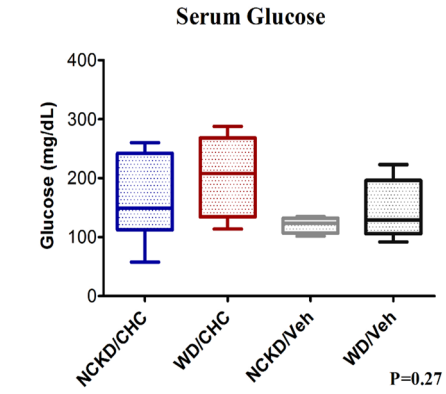

C

D

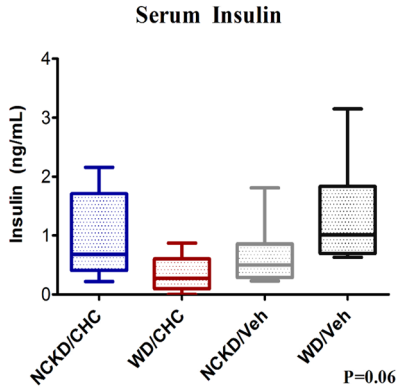

E

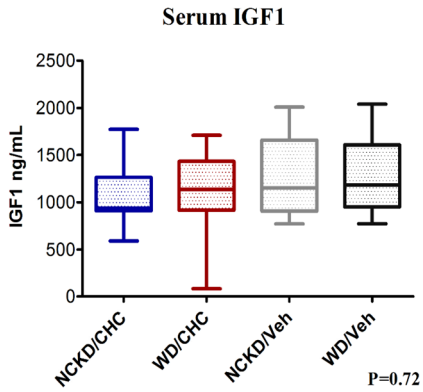

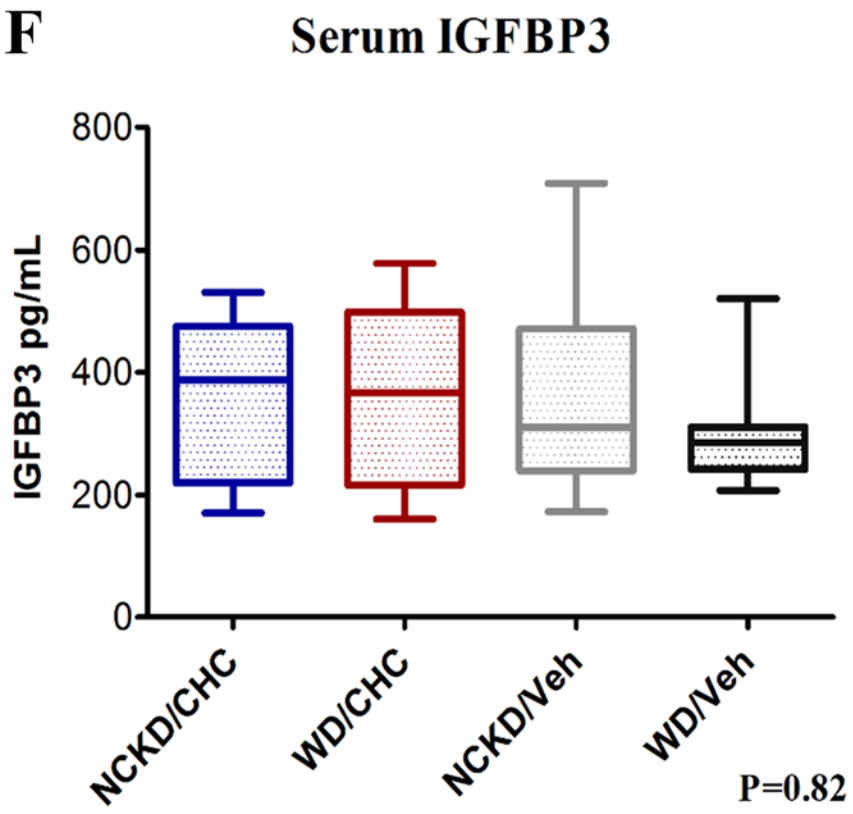

Fig. 9.

Serum hormone concentrations when the mice were killed (Day 53). **A**, Serum lactate by group. **B**, Serum ketones by group. **C**, Serum glucose by group. **D**, Serum insulin by group. **E**, Serum IGF-1 by group**. F,** Serum IGFBP-3 by group. Box represents 25th, 50th, and 75th percentile. Whisker represents 5th and 95th percentile. .